

# SURFACE ANALYSIS OF FEATURES SEEN ON Nb<sub>3</sub>Sn SAMPLE COUPONS GROWN BY VAPOUR DIFFUSION\*

D.L. Hall<sup>†</sup>, T. Arias, P. Cueva, M. Liepe, J.T. Maniscalco, D.A. Muller, R.D. Porter, N. Sitaraman  
Cornell University, Ithaca, NY 14853, USA

## Abstract

As a high-kappa superconductor with a coherence length of 7 nm, the superconductor Nb<sub>3</sub>Sn is highly susceptible to material features at the sub-micron scale. For niobium surfaces coated with a thin layer of Nb<sub>3</sub>Sn using the vapour diffusion method, the polycrystalline nature of the film grown lends to the possibility that performance-degrading non-uniformities may develop. In particular, regions of insufficiently thick coating and tin-depletion have been seen to occur in sample coupons. In the interests of understanding how to control the presence and nature of such features, it is necessary to know how they form. In this paper we stop the coating at defined instances to gain a stop-motion image of the growth of the layer, and use SEM and TEM techniques to image the development of the features seen in previously coated samples. We demonstrate that surface pre-anodisation can suppress the formation of thin film regions, and apply this technique to a single-cell cavity. Contemporarily, we use TEM with EDS mapping to monitor grain boundaries and tin-depleted regions within the layer.

## INTRODUCTION

The A15 superconductor Nb<sub>3</sub>Sn has proven itself to be a promising successor to niobium for use in SRF cavities [1–4]. However, the Nb<sub>3</sub>Sn layer grown using the vapour diffusion process is polycrystalline and rich in surface features, both in terms of topology and composition. In this paper we examine some of the features seen in recent surface analysis studies performed at Cornell University, and discuss them in the light of results from JDFT simulations.

## EXPERIMENTAL METHOD

For reference, SEM images of the Nb<sub>3</sub>Sn surface were taken using a Tescan Mira3 FESEM, equipped with a Bruker Xflash 6|60 EDS detector. TEM images were taken using an FEI F20 TEM/STEM.

### Surface Pre-Anodisation

Surface pre-anodisation is a substrate preparation technique that has been shown [4] to suppress the formation of thin regions of Nb<sub>3</sub>Sn. These are regions of the Nb<sub>3</sub>Sn

\* This work was primarily supported by U.S. DOE award DE-SC0008431. This work was supported in part by the U.S. National Science Foundation under Award PHY-1549132, the Center for Bright Beams. This work made use of the Cornell Center for Materials Research Shared Facilities which are supported through the NSF MRSEC program (DMR-1120296). Travel to IPAC'17 supported by the Division of Physics of the United States National Science Foundation (Accelerator Science Program) and the Division of Beam Physics of the American Physical Society.

<sup>†</sup> dlh269@cornell.edu

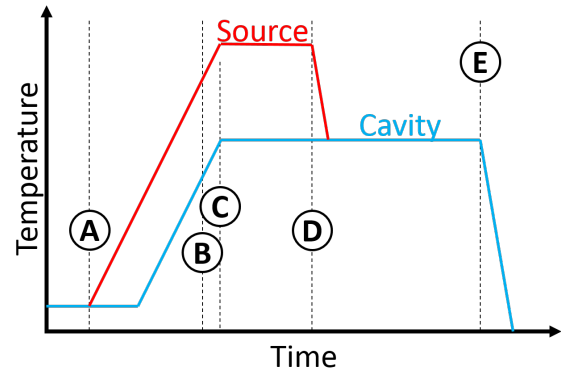


Figure 1: An illustrated version of the coating procedure, showing the points at which the coating was stopped. Specifics are given in the text.

coating that are too thin to effectively screen the niobium substrate from the applied RF field, being only a few hundred nanometres thick, and resulting in greater losses.

Surface pre-anodisation consists of growing the oxide layer of the niobium substrate using electrolytic methods prior to coating in an ultra-high vacuum furnace specially equipped for the task. The niobium is immersed in a bath of 10% w/w NaOH solution, surrounded by a high-purity tin wire electrode. A voltage difference of 30 volts, with the niobium being positive and the tin electrode being negative, is applied while keeping the current density on the niobium electrode at approximately 10-30 mA/cm<sup>2</sup>, allowing the oxide layer to grow to a light sky-blue colour, which corresponds to an oxide thickness of approx. 72 nm. Upon achieving the desired voltage (which is held fixed using a voltage limiter on the power supply), the power is cut and the sample is removed from the bath, whereupon it is cleaned in an ultrasonic bath while immersed in methanol.

### Stop-Motion Coating Series

For the purposes of understanding the growth of the RF layer, a series of coatings were done based upon the current standard coating procedure. However, for each coating, the procedure was interrupted at a different stage in the coating process. A diagram of the coating procedure, shown in Fig. 1, illustrates this. The stopping points performed so far are:

- (A) At the end of the 5 hours nucleation step at 500°C
- (B) At the point at which the chamber reaches a temperature of 950°C
- (C) At the point at which the chamber has reached the coating temperature of 1120°C

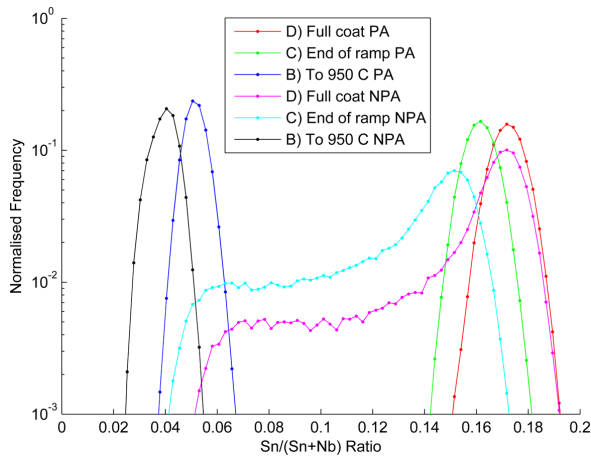


Figure 2: A histogram showing the ratio of the Sn/(Sn+Nb) signal in an EDS map of the Nb<sub>3</sub>Sn surface for different samples, taken from different stages in the coating process. A distinction is made between samples that were pre-anodised (PA) and not pre-anodised (NPA).

- (D) At the end of the coating step of 1.5 hours (therefore omitting the annealing step)
- (E) At the end of the annealing step of 1 further hour.

For each coating, two samples were coated simultaneously, hanging near each other in the furnace. One was anodised to 30 V of oxide layer, whilst the other was untouched, having only its natural passive oxide layer.

### RESULTS FROM SURFACE ANALYSIS STUDIES

For stages (B), (C) and (D), EDS maps of the Nb<sub>3</sub>Sn surface were performed in the SEM at a beam voltage at 30 kV. At these energies, the electron beam has sufficient energy to penetrate through a Nb<sub>3</sub>Sn layer that is less than 500 nm thick, resulting in an excess of Nb signal coming from the bulk. From the EDS map, a histogram of the ratio of intensity, Sn/(Sn+Nb), is obtained from each pixel. Such a histogram is shown for stages (B), (C), and (D), in both pre-anodised and not pre-anodised samples is shown in Fig. 2. In a perfect, stoichiometric layer of sufficient thickness, this will result in a Gaussian shape centred at a ratio of about 0.18. The presence of thin film regions will be revealed as a left-side tail in the Gaussian distribution.

As can be seen, the pre-anodised samples never demonstrate any tail indicative of the presence of thin film regions at any stage during the growth process seen so far. Not only that, but at any one stage, the pre-anodised sample always appears more developed, i.e. thicker, than its non pre-anodised brother. This is corroborated with the SEM images of the Nb<sub>3</sub>Sn surface seen in Fig. 3, which show the coating at the end of stages (A), (B) and (C).

In particular, the end of the nucleation stage shows some marked differences between the pre-anodised sample and

non. The nucleation sites appear significantly larger, although they remained space roughly the same distance apart. Looking forward towards stage (B), the pre-anodised substrate appears considerably more matured than its counterpart, although there appear to be highly defined raised regions scattered across the surface. The equivalent non pre-anodised sample, instead, demonstrates regions that look pimples, surrounded by matte regions reminiscent of the thin film regions seen in fully grown samples. Such a region can be seen in the (C) stage for the non-preanodised sample, to the right of the centre of the image. As expected, no such regions are seen in the pre-anodised sample.

Analysing the transition from a thick to a thin region in a cross-section TEM reveals the disparity in the thickness, as seen in Fig. 4. The cross-section shown was taken from stage (D), at the end of the coating step but omitting the annealing step. The thick region is shown to be approximately 2 microns deep, compared to the thin region which falls down to a mere 200 nm at places. Interestingly, an EDS linescan of the thin film region, going from the RF surface into the bulk, demonstrates a significant excess of un-alloyed

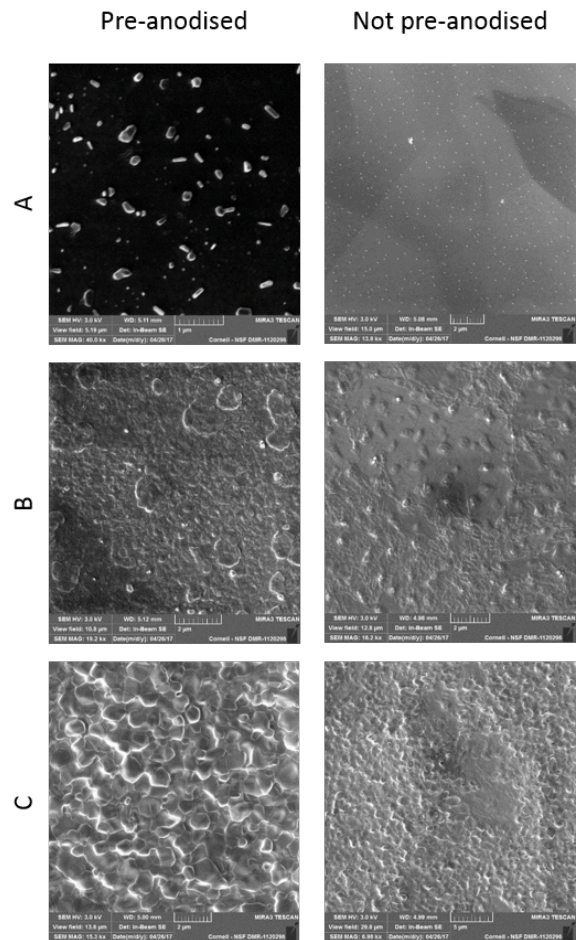
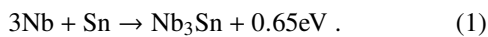


Figure 3: SEM images of the Nb<sub>3</sub>Sn surface during the growth procedure, for coating stages (A), (B) and (C), in both pre-anodised and not pre-anodised samples.

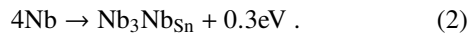
tin at the very surface of the thin film region. This excess is not seen in thicker regions of the film. In EDS maps of the cross-section, tin-depleted regions are seen within the bulk of the Nb<sub>3</sub>Sn layer; the presence of these tin-depleted regions is well-known and has been reported upon previously [5, 6].

## THEORETICAL MODEL OF LAYER GROWTH

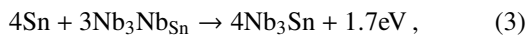
To better understand the mechanisms and dynamics of growth of the Nb<sub>3</sub>Sn layer, Joint Density Functional Theory, in the form of the JDFTx computational framework [7–9], was employed to calculate energies for the reactions that occur during layer growth, including the formation of tin-depleted regions. The process for the formation of Nb<sub>3</sub>Sn from Nb and Sn is given by



This result is in good agreement with calorimetric data [10]. Tin-depletion is the result of a reaction between Nb and Nb<sub>3</sub>Sn. It is energetically favourable for BCC Nb atoms to join the A15 phase, resulting in Nb substitutional defects at Sn sites,



These Nb<sub>Sn</sub> defects are often found near the Nb-Nb<sub>3</sub>Sn interface, but mechanisms exist for them to form elsewhere in the Nb<sub>3</sub>Sn layer as well. Fortunately, the repair of such defects is also energetically favourable,



although as is obvious from the EDS maps, this reaction does not readily repair defects that are not in immediate contact with Sn, at least under current coating conditions.

Calculations performed using density-functional theory confirm that the speed with which the Nb<sub>3</sub>Sn layer grows at our coating temperature is considerably enhanced by the presence of grain boundaries in the Nb<sub>3</sub>Sn layer. These grain boundaries allow elemental tin to move from the surface to the bulk where it is needed to grow the layer. As the layer grows, so too does the average grain diameter, decreasing the density of grain boundaries and significantly slowing the growth of the layer.

The density of grain boundaries is lowest in thin film regions, with the entire thin film region essentially being one large, flat, thin grain. The absence of grain boundaries causes these regions to grow extremely slowly, and also explains the accumulation of un-alloyed tin on the surface of these regions in the absence of an annealing step; without the grain boundaries to adsorb the tin, the uptake of tin into the layer is considerably slower.

## CONCLUSION

A stop-motion coating series has begun to shed light on the difference between the growth of Nb<sub>3</sub>Sn layers of pre-anodised samples whose oxide layer has been thickened and

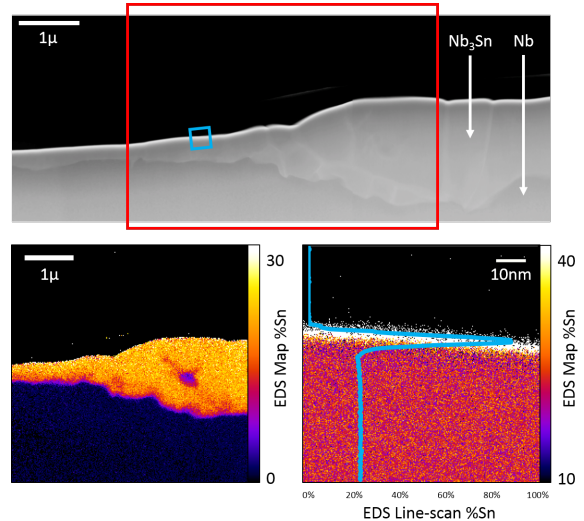


Figure 4: (Top) A TEM cross-section of a Nb<sub>3</sub>Sn layer, taken from a non pre-anodised sample from coating stage (D), showing the transition from a thick polycrystalline region to a thin region devoid of grain boundaries. In (Bottom left) an EDS map of the entire cross-section, we see a tin-depleted region in the thicker section. A detailed line scan (Bottom right) of the surface of the thin film region reveals the presence of un-alloyed tin right at the surface of the sample.

samples that are coated with naught but their natural oxide layer. Simulations with JDFTx confirm that the growth of the Nb<sub>3</sub>Sn layer is mediated primarily via grain boundaries in the already formed layer, such that as the grain boundary density decreases, so too does the speed with which the layer grows. This preference for grain boundary growth also explains the presence of un-alloyed tin on the surface of thin film regions (whose grain boundary density is very low) in samples that received a coating without an annealing step.

## REFERENCES

- [1] D. Hall, J. Kaufman, M. Liepe, R. Porter, and J. Sears, “First results from new single-cell Nb<sub>3</sub>Sn cavities coated at Cornell University”, presented at IPAC’17, Copenhagen, Denmark, May 2017, paper MOOCA2.
- [2] S. Posen and D. Hall, “Nb<sub>3</sub>Sn superconducting radiofrequency cavities: fabrication, results, properties, and prospects”, in *Superconductor Science and Technology*, vol. 30(3), p. 33004, 2017.
- [3] D. Hall, M. Liepe, and J. Maniscalco, “RF measurements on high performance Nb<sub>3</sub>Sn cavities”, in *Proc. of IPAC’16*, paper WEPMR024.
- [4] D. Hall, “Next generation Nb<sub>3</sub>Sn cavities: Current performance, limitations, and considerations for practical use”, presented at the Tesla Technology Collaboration meeting at CEA Saclay, Paris, 2016.
- [5] D. Hall, H. Conklin, T. Gruber, J. Kaufman, J. Maniscalco, M. Liepe, B. Yu, and T. Proslie, “Surface analysis and ma-

terial property studies of Nb<sub>3</sub>Sn on Niobium for use in SRF cavities, in Proc. of SRF'15, paper TUPB045.

- [6] C. Becker, S. Posen, N. Groll, R. Cook, C. Schlepütz, D. Hall, M. Liepe, M. Pellin, J. Zasadzinski, and T. Proslie, “Analysis of Nb<sub>3</sub>Sn surface layers for superconducting radio frequency cavity applications”, Applied Physics Letters, vol. 106(8), p. 082602, February 2015.
- [7] R. Sundararaman, D. Gunceler, K. Letchworth-Weaver, K. Schwarz, and T. Arias, JDFTx (<http://jdf.tx.org/>), 2012.
- [8] S. Ismail-Beigi and T. Arias, “New algebraic formulation of density functional calculation”, in Computer Physics Communications, vol. 128(1), p. 1–45, 2000.
- [9] T. Arias, M. Payne and J. Joannopoulos, “Ab initio molecular dynamics: Analytically continued energy functionals and insights into iterative solutions”, Phys. Rev. Lett., vol. 69(7), pp. 1077–1080, August 1992.
- [10] C. Toffolon, C. Servant, J. Gachon, and B. Sundman, “Re-assessment of the Nb-Sn system”, Jour. of Phase Equilibria, vol. 23(2), p. 134, 2002.